ECCOMAS Congress 2016
VII European Congress on Computational Methods in Applied Sciences and Engineering
M. Papadrakakis, V. Papadopoulos, G. Stefanou, V. Plevris (eds.)
Crete Island, Greece, 5–10 June 2016

A CHEBYSHEV INTERPOALTION-BASED FAST MULTIPOLE METHOD FOR POROELASTICITY

Barbara Knöbl[1], **Thomas Traub**[1], **and Martin Schanz**[1]

[1] Institute of Applied Mechanics, Graz University of Technology
Technikerstraße 4/II, 8010 Graz, Austria
e-mail: {barbara.knoebl, thomas.traub, m.schanz}@tugraz.at

Keywords: Boundary Element Method, Fast Multipole Method, Poroelasticity, Chebyshev polynomials.

Abstract. *The treatment of porous media with the BEM exhibits some problems, which are common also for the Finite Element Method, but also some BEM specific ones. The three main problems are: First, the multiphase system requires four degrees of freedom per node, leading to large matrices even for small problems. Since the BEM matrices are densely populated, this makes the method prohibitive for large problem sizes. Second, due to the different physical nature of the degrees of freedom the matrix entries vary over several orders of magnitude. Third, the fundamental solution of poroelasticity is computationally expensive.*

We present a FM-BEM that circumvents those points: The Chebyshev interpolation-based FMM significantly reduces the memory consumption of the system matrix and thus allows for larger problem sizes to be treated. As well, it requires fewer evaluations of the fundamental solution. To employ an iterative solver, the use of a transformation of the material data is mandatory.

1 INTRODUCTION

Porous media occur frequently in nature as well as construction materials; probably the best-known example for a natural porous medium is soil. The understanding of wave propagation in such media is of distinct interest for oil and gas explorisation but also for earthquake analysis. In these particular fields the treatment of unbounded domains, such as a halfspace, is required. The Boundary Element Method (BEM) is advantageous over the Finite Element Method (FEM) for the numerical treatment of such geometries, since it requires only the discretisation of the boundary and inherently fulfills the radiation condition [1].

In the most straightforward description the saturated porous media problem shows six unknowns, i.e. the solid's and fluid's displacements $\mathbf{u}$ and $\mathbf{u}^f$, respectively. The description can be reduced to four, using the fluid's pressure p instead of its displacements $\mathbf{u}^f$, which is only possible in the Laplace domain. The BEM requires the knowledge of the fundametal solution of the underlying partial differential equation, which is accordingly also solely available in the Laplace domain. To derive the temporal behavior the Convolution Quadrature Method [2, 3] can be employed.

A review of poroelastic models and their numerical treatment is given in [4]. Early BEM formulations were given by Manolis and Beskos, who presented an $(\mathbf{u}, \mathbf{u}^f)$-description in Laplace domain, and by Cheng et al. [5] and Domínguez [6], publishing frequency domain $(\mathbf{u}, p)$-formulations. An extensive discussion of the collocation BEM for linear poroelasticity is given by Schanz [7]. A symmetric Galerkin BEM, which is advantageous for FEM-BEM-Coupling, was presented in [8].

The application of so-called fast methods is necessary for the efficient treatment of the porous media problem with BEM for the following two reasons: The complicated structure of the fundamental solution makes the evaluation of the matrix entries computationally expensive, and the multiphase system requires four degrees of freedom per node, leading to large matrices even for small problems. Furthermore, it is well known that the BEM matrices are densely populated. Hence, methods are needed that reduce memory and the number of function evaluations; so-called blackbox methods would be preferable. The most promising candidates are the Adaptive Cross Approximation (ACA) [9] and the Fast Multipole Method (FMM). The classical FMM [11] uses an expansion into spherical harmonics to construct a separable expansion of the kernel function. A review of the application of the FMM in BEM is given in [12]. Regarding vector-valued problems, elastodynamics has been successfully treated with the classical FMM, e.g. in [13, 14]. Among the FMM variants the Chebyshev interpolation FMM [10] seems to be favorable for poroelasticity, since the fundamental solution is only evaluated at a small set of spatial points, avoiding an analytical expansion.

In this paper we present a Chebyshev interpolation-based FM-BEM for poroelasticity. In the next section, we briefly summarize the BEM formulation for poroelasticity in Laplace domain. Then we describe the employed Chebyshev interpolation-based FMM where we focus on the differences to the standard FMM. Finally we present numerical experiments to validate the presented algorithms and to demonstrate their advantage over the standard BEM.

2 BOUNDARY ELEMENT FORMULATION IN LAPLACE DOMAIN

In this work we study the linearized behavior of a porous medium saturated with one fluid in the open domain $\Omega \subset \mathbb{R}^3$. In the following we give a brief summary of the problem at hand. A detailed dicussion of Biot's theory [15] and a BEM formulation thereof can be found in [7].

The governing equations of the poroelastic problem are stated for the solid's displacement $\mathbf{u}$

and the fluid's pressure p and read as

$$\mathcal{L}\mathbf{u}^g(\mathbf{x}) = 0 \tag{1}$$

where $\mathbf{u}^g = (\mathbf{u}, p)^\top$ and

$$\mathcal{L} = \begin{bmatrix} \mathcal{L}^S + s^2(\rho - \beta\rho^f)\mathbf{I} & (\alpha - \beta)\nabla \\ s(\alpha - \beta)\nabla^\top & \frac{\beta}{s\rho^f}\nabla^2 + \frac{s\phi^2}{R} \end{bmatrix}. \tag{2}$$

$\mathcal{L}^S$ is the differential operator of the linear elastodynamic problem, $s \in \mathbb{C}, \Re(s) > 0$ is the Laplace parameter, β is defined as

$$\beta = \frac{\kappa\rho^f\phi^2 s}{\phi^2 + s\kappa\left(0.66\,\phi\rho^f + \phi\rho^f\right)}. \tag{3}$$

The remaining symbols are material parameters listed in Table 1.

ρ	density	2458	$[\mathrm{kg/m^3}]$
ρ^f	density of the fluid	1000	$[\mathrm{kg/m^3}]$
α	Biot parameter	0.778	$[\mathrm{N/m^2}]$
R	Biot parameter	$4.885 \cdot 10^8$	$[\mathrm{N/m^2}]$
ϕ	porosity	0.19	$[-]$
λ	Lamé parameter	0	$[\mathrm{N/m^2}]$
μ	Lamé parameter	$7.2 \cdot 10^9$	$[\mathrm{N/m^2}]$
κ	permeability	$1.9 \cdot 10^{-10}$	$[\mathrm{N/m^2}]$

Table 1: Material parameters of Berea sandstone [16]

In this paper we focus on the examination of the different BEM operators which are needed to solve a mixed boundary value problem (BVP) through the so-called direct approach. For simplicity we restrict ourselves to the Dirichlet problem, i.e.

$$\mathbf{u}^g(\mathbf{x}) = \mathbf{g}^D \quad \forall \mathbf{x} \in \Gamma, \tag{4}$$

where $\Gamma = \partial\Omega$.

A solution $\mathbf{u}^g(\mathbf{x})$ for $\mathbf{x} \in \Omega$ can be constructed by the indirect Single-Layer-Potential (SLP) approach

$$\mathbf{u}^g(\mathbf{x}) = \int_\Gamma \left(\mathbf{U}^*(\mathbf{x}, \mathbf{y})\right)^\top \mathbf{w}(\mathbf{y}) ds_\mathbf{y} \quad \forall \mathbf{x} \in \Omega, \tag{5}$$

or by the indirect Double-Layer-Potential (DLP) approach

$$\mathbf{u}^g(\mathbf{x}) = \int_\Gamma \left(\mathcal{T}_y^* \mathbf{U}^*(\mathbf{x}, \mathbf{y})\right)^\top \mathbf{v}(\mathbf{y}) ds_\mathbf{y} \quad \forall \mathbf{x} \in \Omega, \tag{6}$$

where the traction operator is defined as

$$\mathcal{T}_y^* = \begin{bmatrix} \mathcal{T}_y^S & s\,\alpha\mathbf{n}_y \\ -\beta\mathbf{n}_y^\top & \frac{\beta}{s\rho^f}\frac{\partial}{\partial\mathbf{n}_y}. \end{bmatrix} \tag{7}$$

with the traction operator $\mathcal{T}_y^S$ of elasicity. The corresponding boundary integral equation (BIE) for the unknown densities $\mathbf{w}(\mathbf{x})$, $\mathbf{v}(\mathbf{x})$ reads as

$$\mathbf{u}^g(\mathbf{x}) = \int_\Gamma \left(\mathbf{U}^*(\mathbf{x},\mathbf{y})\right)^\top \mathbf{w}(\mathbf{y}) ds_\mathbf{y} \quad \forall \mathbf{x} \in \Gamma \tag{8}$$

and

$$\mathbf{u}^g(\mathbf{x}) = \int_\Gamma \left(\mathcal{T}_y^* \mathbf{U}^*(\mathbf{x},\mathbf{y})\right)^\top \mathbf{v}(\mathbf{y}) ds_\mathbf{y} + (\sigma - 1)\mathbf{v}(\mathbf{x}) \quad \forall \mathbf{x} \in \Gamma, \tag{9}$$

where $\sigma = 0.5$ almost everywhere. The function $\mathbf{U}^*(\mathbf{x},\mathbf{y})$ is the *fundamental solution* of the differential equation, i.e. the Green's function of the adjoint operator $\mathcal{L}^*$. It is a four-by-four-tensor-valued function, where

$$\mathbf{U}^*(\mathbf{x},\mathbf{y}) = \begin{bmatrix} U^S & U^f \\ P^S & P^f \end{bmatrix} \tag{10}$$

with U^S being a three-by-three tensor, U^f a three-by-one tensor, P^s a one-by-three tensor and P^f a scalar. The explicit expressions of the four subblocks can be found in [7].

To achieve a numerical solution of the unknown densities $\mathbf{w}(\mathbf{x})$, $\mathbf{v}(\mathbf{x})$, we approximate $\mathbf{w}(\mathbf{x})$ using constant discontinuous functions φ^0 on a partition of the boundary (triangulation)

$$\mathbf{w}(\mathbf{x}) \approx \sum_{j=1}^{N} \varphi_j^0(\mathbf{x})\, \mathbf{w}_j \tag{11}$$

and $\mathbf{v}(\mathbf{x})$ using linear continous functions φ^1

$$\mathbf{v}(\mathbf{x}) \approx \sum_{j=1}^{M} \varphi_j^1(\mathbf{x})\, \mathbf{v}_j, \tag{12}$$

respectively. Note that for the vector valued problem at hand, the coefficients $\mathbf{w}_j$ and $\mathbf{v}_j$ are accordingly vector valued. The supports of the functions are restricted to either one or some neighboring triangulation elements. Hence, the boundary integral equation can be reformulated to its discretized form

$$\mathbf{u}^g(\mathbf{x}) = \sum_{j=1}^{N} \int_{supp(\varphi_j^0)} \left(\mathbf{U}^*(\mathbf{x},\mathbf{y})\right)^\top \varphi_j^0(\mathbf{y}) ds_\mathbf{y}\, \mathbf{w}_j \quad \forall \mathbf{x} \in \Gamma \tag{13}$$

and

$$\mathbf{u}^g(\mathbf{x}) = \sum_{j=1}^{M} \int_{supp(\varphi_j^1)} \left(\mathcal{T}_y^* \mathbf{U}^*(\mathbf{x},\mathbf{y})\right)^\top \varphi_j^1(\mathbf{y}) ds_\mathbf{y}\, \mathbf{v}_j + (\sigma - 1)\varphi_j^1(\mathbf{x})\mathbf{v}_j \quad \forall \mathbf{x} \in \Gamma, \tag{14}$$

respectively. This yields $N(M)$ vector-valued unknowns $\mathbf{w}_j$ ($\mathbf{v}_j$). The collocation method is employed to solve the BIE for the unknown coefficients: The equation is evaluated for N (M) $\mathbf{x}_i \in \Gamma$, yielding a set of equations for $\mathbf{w}$

$$\mathbf{u}^g(\mathbf{x}_i) = \sum_{j=1}^{N} \int_{supp(\varphi_j^0)} \left(\mathbf{U}^*(\mathbf{x}_j,\mathbf{y})\right)^\top \varphi_j^0(\mathbf{y}) ds_\mathbf{y}\, \mathbf{w}_j =: \mathbf{V}_{ij}\, \mathbf{w}_j \tag{15}$$

and $\mathbf{v}$

$$\mathbf{u}^g(\mathbf{x}_i) = \sum_{j=1}^{M} \int_{supp(\varphi_j^1)} \left(\mathcal{T}_y^* \mathbf{U}^*(\mathbf{x}_i, \mathbf{y})\right)^\top \varphi_j^1(\mathbf{y}) ds_\mathbf{y}\, \mathbf{v}_j + (\sigma - 1)\varphi_j^1(\mathbf{x}_i)\mathbf{v}_j \tag{16}$$

$$=: \left(\mathbf{K}_{ij} + (\sigma - 1)\mathbf{I}\right)\, \mathbf{v}_j, \tag{17}$$

Note that the indices i, j refer to four-by-four blocks (*block entry*) of the fundamental solution and to a subvector $\mathbf{w}_i$ of lentgh four.

The system matrix $\mathbf{V}_{ij}$ ($\mathbf{K}_{ij}$) is densely populated and hence, the standard collocation BEM scales quadratically in the number of unknowns. It can be solved using a direct solver, which scales like N^3 (M^3), or by means of an iterative solver, which involves a matrix-vector-product (MVP) in each iteration, scaling quadratically, while the number of iterations may be kept approximately constant with respect to N (M) when using a preconditioner [1].

For the measured material data of Berea sandstone [16], c.f. Table 1, the entries of the system matrix $\mathbf{V}_{ij}$ ($\mathbf{K}_{ij}$) differ by magnitudes. Numerical tests show that the direct solver employed (Eigen's `PartialPivLU` [17]) indeed yields an accurate solution of the resulting ill-conditioned system. The use of iterative solvers, on the other hand, requires a better conditioning and is mandatory for the use of fast methods like the FMM.

Numerical tests show that a simple transformation of the material data as described in [18] is sufficient to achieve that, i.e.

$$\tilde{x}_i = \frac{x_i}{A} \quad \tilde{t} = \frac{t}{B} \quad \tilde{\lambda} = \frac{\lambda}{C} \quad \tilde{\mu} = \frac{\mu}{C} \quad \tilde{\rho} = \frac{A^2}{B^2\, C}\rho \quad \tilde{\kappa} = \frac{B\, C}{A^2}\kappa \tag{18}$$

with $A = 1$, $B = 1$, $C = \mu(3\lambda + 2\mu)/(\lambda + mu)$.

Similar to iterative solvers, compression methods like the truncated Singular Value Decomposition (SVD) are likewise sensitive to such differing matrix entries, whereas the use of the transformed material data allows for its immediate application. Hence, in the following, we use the transformed material data for all calculations.

3 INTERPOLATION-BASED FM-BEM FOR POROELASTICITY

Solving (15) for $\mathbf{w}_j$ using an iterative solver involves evaluating the matrix-vector-product many times. The basic idea of the FMM is to construct a fast summation scheme by the use of a separable expansion (often denoted "degenerate expansion") of the considered function.

The FMM used in this paper is a Chebyshev interpolation-based FMM based on the *black-box FMM* by Darve [10]. In the case of the BEM the considered function is the discretized boundary integral operator $\mathbf{V}_{ij}$, or $\mathbf{K}_{ij}$, respectively. Thus, it involves the integration over the function at hand. A separable expansion of the fundamental solution allows to shift its evaluation outside the integral. Such an expansion is only possible for distant points $\mathbf{x}, \mathbf{y}$, i.e. for off-diagonal blocks of the system matrix. Therefore the standard geometrical clustering scheme of the FMM [11] is employed. For the FM-BEM we cluster over the collocation points, which is straightforward, and over the shape functions. Because of the strictly geometrical clustering the supports of some shape functions are not entirely enclosed within the cluster's boundaries. Thus the cluster's bounding box is extended such that the supports are just enclosed within.

Before we describe the different FM-operators, we briefly summarize the Chebyshev interpolation of an arbitrary function $f : \mathbb{R} \to \mathbb{C}$,

$$f(x) \approx \sum_{m=1}^{p} S_p(\bar{x}_m, x)\, f(\bar{x}_m). \tag{19}$$

The interpolation function $S_p(\bar{x}_m, x)$ is defined on the interval $[-1, 1]$ and reads as

$$S_p(\bar{x}_m, x) = \frac{1}{p} + \frac{2}{p} \sum_{n=1}^{p-1} T_n(x)\, T_n(\bar{x}_m) \quad \forall x \in [-1, 1]. \tag{20}$$

It can easily be extended to arbitrary intervals using a linear transformation. $T_n(x)$ denote the Chebyshev polynomials of order p,

$$T_n(x) = \cos(n \, \arccos(x)) \quad \forall x \in [-1, 1], \tag{21}$$

and $\bar{x}_m$ the corresponding roots,

$$\bar{x}_m = \cos\left(\frac{(m - \frac{1}{2})\pi}{p}\right). \tag{22}$$

For the sake of readability we do not distinct between the standard interpolation function and its transformed variant and denote both $S_p(\bar{x}_m, x)$, since it is clear from the context which one is used. This interpolation scheme can easily be extended to functions on $\mathbb{R}^3$ using

$$S_p(\bar{\mathbf{x}}_\mathbf{m}, \mathbf{x}) = \prod_{i=1}^{3} S_p(\bar{x}_{m_i}, x_i), \tag{23}$$

where $\bar{\mathbf{x}}_m = (\bar{x}_{m_1}, \bar{x}_{m_2}, \bar{x}_{m_3})$ and $\mathbf{m}$ is a multi-index. The straightforward way to approximate non-scalar functions like the tensor-valued fundamental solution $\mathbf{U}^*(\mathbf{x}, \mathbf{y})$ is to interpolate all entries using the same intepolation scheme, which is equivalent to multiplying the whole block with the scalar interpolation function S_p.

We concentrate on the differences between the standard FMM and the FM-BEM and hence omit the description of the multilevel scheme which can be found in [11]. To illustrate the method we present the idea of the Chebyshev interpolation-based FMM for one block entry of the discretized SLP operator

$$\mathbf{V}_{ij} = \int_{supp(\varphi_j^0)} \left(\mathbf{U}^*(\mathbf{x}_i, \mathbf{y})\right)^\top \varphi_j^0(\mathbf{y}) ds_\mathbf{y}\,. \tag{24}$$

Interpolation with respect to $\mathbf{y}$ yields

$$\mathbf{V}_{ij} = \sum_\mathbf{m} \left(\mathbf{U}^*(\mathbf{x}_i, \bar{\mathbf{y}}_\mathbf{m})\right)^\top \underbrace{\int_{supp(\varphi_j^0)} S_p(\bar{\mathbf{y}}_\mathbf{m}, \mathbf{y}) \varphi_j^0(\mathbf{y}) ds_\mathbf{y}}_{\text{P2M-operator}}\,. \tag{25}$$

Further, interpolation with respect to $\mathbf{x}$ yields

$$\mathbf{V}_{ij} = \underbrace{\sum_\mathbf{n} S_p(\mathbf{x}_i, \bar{\mathbf{x}}_\mathbf{m})}_{\text{L2P-operator}} \underbrace{\sum_\mathbf{m} \left(\mathbf{U}^*(\bar{\mathbf{x}}_\mathbf{n}, \bar{\mathbf{y}}_\mathbf{m})\right)^\top}_{\text{M2L-operator}} \int_{supp(\varphi_j^0)} S_p(\bar{\mathbf{y}}_\mathbf{m}, \mathbf{y}) \varphi_j^0(\mathbf{y}) ds_\mathbf{y}\,. \tag{26}$$

The points $\bar{\mathbf{x}}_\mathbf{n}, \bar{\mathbf{y}}_\mathbf{m} \in \mathbb{R}^3$ are the three-dimensional Chebyshev nodes transformed to the bounding box. Obviously, using such an interpolation, the number of kernel evaluations can be reduced if the submatrix associated with the corresponding clusters of $\mathbf{x}_i$ and φ_j^0 is larger than

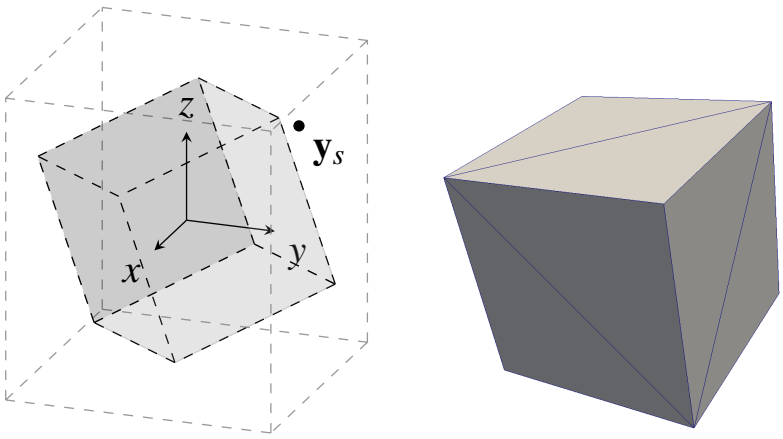

(a) domain and source point (b) coarsest mesh

Figure 1: Computation domain.

the associated M2L-operator of size $p^3 \times p^3$. The reduction is actually significantly larger, since for the numerical integration in the standard BEM (15) the kernel is evaluated for each quadrature point. Using the FMM this integration arises in the P2M-operator, which involves only the numerical integration of a polynomial. We emphasize that the matrix approximation is implemented in terms of MVPs, and that an aforementioned multi-level scheme is used.

The traction fundamental solution explicitly depends on the normal vector of an associated surface, i.e. on the normal vector of the triangulation element in the case of the discretized boundary integral operator. Hence a direct interpolation as presented for the SLP is not possible. Recalling (16) the DLP operator is defined as

$$\mathbf{K}_{ij} = \int_{supp(\varphi_j^1)} \left(\mathcal{T}_y^* \mathbf{U}^*(\mathbf{x}_i, \mathbf{y})\right)^\top \varphi_j^1(\mathbf{y}) ds_\mathbf{y} \tag{27}$$

and can thus be interpolated using the interpolation of $\mathbf{U}^*$

$$\mathbf{K}_{ij} = \sum_\mathbf{m} \left(\mathbf{U}^*(\mathbf{x}_i, \bar{\mathbf{y}}_\mathbf{m})\right)^\top \int_{supp(\varphi_j^1)} \left(\mathcal{T}_y^{*\top} S_p(\bar{\mathbf{y}}_\mathbf{m}, \mathbf{y})\right) \varphi_j^1(\mathbf{y}) ds_\mathbf{y}. \tag{28}$$

The traction operator $\mathcal{T}_y^*$ can be shifted onto the interpolation functions, which leads to a tensorial interpolation operator, whereas all other operations are identical to the SLP. Hence, the calculation of the far field of the DLP-operator only involves the evalution of the fundametal solution $\mathbf{U}^*$ itself.

4 NUMERICAL EXAMPLES

To study the FMM for the poroelastic problem we seek a numerical solution of a known solution to the homogenous differential equation. For a source point $\mathbf{y}_s$ outside the domain, the individual rows of the fundamental solution $\mathbf{U}^*(\mathbf{x}, \mathbf{y}_s)$ fulfill (1) and thus we use a linear combination of all rows as boundary condition. To study a general case, the calculation domain is a unit cube which is rotated along the axes of the coordination system, c.f. Figure 1.

We create a sequence of triangulations by global uniform refinement starting at the coarsest discretization using 12 elements as depicted in Figure 1, denoted Level 0.

All computations are performed using our in-house developed C++ library HyENA. The dense computations are solved using Eigen's `PartialPivLU` [17], the FMM computations

using AHMED's `FGMRes` [19]. Further, the M2L-operators are compressed using the Singular Value Decomposition of LAPACK, and OpenMP is used for parallelization. All computation parameters are listed in Table 2.

The mean error of the computation is determined using (5). It is evaluated for a set of 27 points in the interior of the box $[-\mathbf{0.01}, \mathbf{0.01}] \subset \mathbb{R}^3$ in the center of the computation domain. We compare the inner error of the FM-BEM to the dense calclulation to find the required minimal interpolation order, which turns out to be $p = 4$ for Level 3. The errors are listed in Tables 3 (SLP) and 4 (DLP). We note that for the finest mesh (Level 6), where a comparision with a dense computation is not possible, the order of convergence (eoc) of the SLP approach deviates from its assumed value of 2. The convergence of the coarser levels exceeds that value, which might explain this deviation.

	SLP					DLP				
Mesh level	N	L	p	ϵ_{SVD}	N_{it}	M	L	p	ϵ_{SVD}	N_{it}
3	3072	2	4	10^{-4}	30	1544	2	4	10^{-4}	15
4	12288	3	5	10^{-5}	38	6152	3	5	10^{-5}	18
5	49152	4	6	10^{-6}	48	24584	4	6	10^{-6}	19
6	196608	5	7	10^{-7}	61	98312	5	7	10^{-7}	20

Table 2: Indirect SLP, DLP: computation parameters

	displacement				pressure			
Mesh level	ϵ_{dense}	eoc	ϵ_{FM}	eoc	ϵ_{dense}	eoc	ϵ_{FM}	eoc
3	2.306E-4		2.358E-4		4.388E-4		4.350E-4	
4	4.018E-5	2.52	3.957E-5	2.57	7.904E-5	2.47	7.859E-5	2.47
5	7.363E-6	2.45	7.126E-6	2.47	1.458E-5	2.44	1.405E-5	2.48
6	-	-	3.193E-6	1.16	-	-	5.063E-6	1.47

Table 3: Indirect SLP: mean relative inner error

	displacement				pressure			
Mesh level	ϵ_{dense}	eoc	ϵ_{FM}	eoc	ϵ_{dense}	eoc	ϵ_{FM}	eoc
3	9.224E-4		9.487E-4		4.333E-4		4.417E-4	
4	2.311E-4	2.00	2.376E-4	2.00	9.981E-5	2.12	1.038E-4	2.09
5	6.270E-5	1.88	6.270E-5	1.92	2.228E-5	2.16	2.387E-5	2.12
6	-	-	1.495E-5	2.07	-	-	1.113E-5	1.10

Table 4: Indirect DLP: mean relative inner error

Further, we analyze the memory requirement of the FM-BEM. It is calculated by the total size of all FMM operators. Comparision with the dense operators yields the compression of the FM-BEM. Table 5 lists the memory requirement, its scaling with respect to refinement and the compression.

The classical FMM scales linearly in N/M for constant interpolation order p. To preserve the convergence of the inner error the interpolation order p needs to be increased for each refinement

	SLP					DLP				
Mesh level	M_{dense}	scal.	M_{FM}	scal.	compr.	M_{dense}	scal.	M_{FM}	scal.	compr.
3	0.15		0.17		115%	0.04		0.07		186%
4	2.42	2.00	1.22	1.41	51%	0.61	1.99	1.12	1.99	185%
5	38.65	2.00	4.65	0.96	12%	9.67	2.00	4.64	1.02	48%
6	618.48	2.00	15.25	0.86	2%	154.64	2.00	14.13	0.80	9%

Table 5: Indirect SLP, DLP: memory requirement M[GB] and compression

and, hence, this scaling cannot be achieved. Still, the memory consumption of the FM-BEM scales better than the dense computation and is close to 1. The measured scalings below 1 arise from the compression of the M2L-operators using SVD. The indirect SLP collocation FM-BEM requires less memory than the dense case from refinement level 4 upwards, with a compression of 51% and better. The indirect DLP collocation FM-BEM achieves a compression below 1 for levels 5 and higher. The validity of the FM-BEM is confirmed by the convergence of the inner error.

5 CONCLUSION

The presented FM-BEM circumvents three major problems of the standard BEM for poroelasticity: First, using the Chebyshev interpolation-based FMM, the number of evaluations of the computationally expensive fundamental solution $\mathbf{U}^*(\mathbf{x}, \mathbf{y})$ is significantly reduced. Second, for large problems, the storage requirement of the FM-BEM operators is much smaller than for the dense operators. A significant compression, though, was only achieved using the SVD to compress the M2L-operators.

Third, the different physical natures of the unknowns lead to system matrices whose entries vary over several orders of magnitude. The Chebyshev interpolation is insensitive to such varying magnitudes, and numerical tests show that even for the untransformed material, this most simple interpolation yields similar relative errors for all four matrix blocks. The use of an iterative solver, however, requires the use of the transformed material data as described in Section 2. Finally, the accuracy of the presented FM-BEM is mirrored by the convergence of the mean inner error.

REFERENCES

[1] O. Steinbach, *Numerical Approximation Methods for Elliptic Boundary Value Problems*. Springer New York, 2008.

[2] C. Lubich, Convolution quadrature and discretized operational calculus I. *Numer, Math.*, **52**, 129-145, 1988.

[3] C. Lubich, Convolution quadrature and discretized operational calculus II. *Numer, Math.*, **52**, 413-425, 1988.

[4] M. Schanz, Poroelastodynamics: Linear Models, Analytical Solutions, and Numerical Methods. *App. Mech. Rev.*, **62**, 030803-1 - 030803-15, 2009.

[5] A. H.-D. Cheng, T. Badmus, and D. Beskos, Integral Equations for Dynamic Poroelasticity in Frequency Domain With BEM Solution. *J. Eng. Mech.*, **117**, 1136-1157, 1991.

[6] J. Domínguez, Boundary Element Approach for Dynamic Poroelastic Problems. *Int. J. Numer. Methods Eng.*, **35**, 307-324, 1992.

[7] M. Schanz, *Wave Propagation in Viscoelastic and Poroelastic Continua. A Boundary Element Approach*, volume 2 of *Lecture notes in applied mechanics*. Springer, 2001.

[8] M. Messner and M. Schanz, A Symmetric Galerkin Boundary Element Method for 3d Linear Poroelasticity. *Acta Mech.*, **223**, 1751-1768, 2012.

[9] M. Bebendorf, Approximation of boundary element matrices. *Numer. Math.*, **86**, 565-589, 2000.

[10] W. Fong and E. Darve, The black-box fast multipole method. *J. Comp. Phys.*, **228**, 8712-8725, 2009.

[11] L. Greengard and V. Rokhlin, A fast algorithm for particle simulations. *J. Comp. Phys.*, **73**, 325-348, 1987.

[12] N. Nishimura, Fast multipole accelerated boundary integral equation methods. *Appl. Mech. Rev.*, **55**, 299-324, 2002.

[13] H. Fujiwara, The fast multipole method for solving integral equations of three-dimensional topography and basin problems, *Geophys. J. Int.* **140**, 198-210, 2000.

[14] S. Chaillat, M. Bonnet and J.-F. Semblat, A multi-level fast multipole BEM for 3-d elastodynamics in the frequency domain. *Comput.Methods in Appl.Mech.Eng.* **197** 4233-4249, 2008.

[15] M. A. Biot, Theory of propagation of elastic waves in a fluid-saturated porous solid I: Low-frequency range. *J. Acoust. Soc. Am.*, **28**, 168-178, 1956.

[16] Y. K. Kim and H. B. Kingsbury, Dynamic Characterization of Poroelastic Materials. *Exp. Mech.*, **19**, 252-258, 1979.

[17] G. Guennebaud and B. Jacob, Eigen v3. http://eigen.tuxfamily.org, 2010.

[18] M. Schanz and L. Kielhorn, Dimensionless Variables in a Poroelastodynamic Time Domain. *Building Research Journal* **53**, 175-189, 2005.

[19] M. Bebendorf. Another software library on hierarchical matrices for elliptic differential equations (AHMED). http://bebendorf.ins.uni-bonn.de/AHMED.html, 2008.